

---

# PERSONALIZED PATE: DIFFERENTIAL PRIVACY FOR MACHINE LEARNING WITH INDIVIDUAL PRIVACY GUARANTEES

---

**Christopher Mühl**

Freie University Berlin  
christopher.muehl@fu-berlin.de

**Franziska Boenisch**

Fraunhofer AISEC Institute  
franziska.boenisch@aisec.fraunhofer.de

## ABSTRACT

Applying machine learning (ML) to sensitive domains requires privacy protection of the underlying training data through formal privacy frameworks, such as differential privacy (DP). Yet, usually, the privacy of the training data comes at the costs of the resulting ML models' utility. One reason for this is that DP uses one homogeneous privacy budget  $\epsilon$  for all training data points, which has to align with the strictest privacy requirement encountered among all data holders. In practice, different data holders might have different privacy requirements and data points of data holders with lower requirements could potentially contribute more information to the training process of the ML models. To account for this possibility, we propose three novel methods that extend the DP framework Private Aggregation of Teacher Ensembles (PATE) to support training an ML model with different personalized privacy guarantees within the training data. We formally describe the methods, provide theoretical analyses of their privacy bounds, and experimentally evaluate their effect on the final model's utility at the example of the MNIST and Adult income datasets. Our experiments show that our personalized privacy methods yield higher accuracy models than the non-personalized baseline. Thereby, our methods can improve the privacy-utility trade-off in scenarios in which different data holders consent to contribute their sensitive data at different privacy levels.

**Keywords** Differential Privacy, Machine Learning, Private Aggregation of Teacher Ensembles, Personalized Privacy

## 1 Introduction

Machine Learning (ML) is being applied to an increasing number of sensitive domains, such as health care [1, 2], genetics and genomics [3], or hiring processes [4]. Therefore, insuring privacy of the data that the ML models are trained on plays an increasingly vital role. Yet, research has shown that ML models are prone to privacy attacks [5, 6, 7]. Such attacks allow malicious adversaries to learn what data points the ML model under attack has been trained on, what sensitive attributes the data exhibits, or how the data is distributed.

One gold standard to protect data privacy is the mathematical framework of Differential Privacy (DP) [8]. It allows to learn potentially sensitive properties about a population of data as a whole while disclosing limited private information about individual data points. This is achieved through applying a controlled amount of statistical noise on the data or during the analysis in order to dissimulate sensitive properties. The amount of noise to be added depends on a so called privacy budget  $\epsilon$ . Lower values of  $\epsilon$  produce higher amounts of noise that guarantee high privacy but potentially reduce utility [9, 10].

Currently, there exist two broad approaches to apply DP to ML models, namely the Differentially Private Stochastic Gradient Descent (DP-SGD) algorithm [11], and the Private Aggregation of Teacher Ensembles (PATE) framework [12]. The former approach performs the noise addition according to the privacy budget  $\epsilon$  in the ML training procedure. The latter one adds noise during a knowledge transfer from models that were non-privately trained on sensitive data to another model with privacy guarantees. In both cases, the amount of sensitive information that the trained ML models can potentially leak at inference time is bounded according to a privacy budget  $\epsilon$  that is specified for the whole dataset.

However, in reality, different data holders might require different levels of privacy for their data points. To account for all data points' privacy needs, the privacy budget  $\epsilon$  of an application, therefore, must comply with the highest

privacy requirement (lowest  $\epsilon$ ) encountered among all of them. Given the privacy-utility trade-off mentioned above, it would, however, be desirable to allow for several personalized privacy budgets among data point within a DP-based ML model training. This would make it unnecessary to always choose the lowest  $\epsilon$  and thereby potentially allow for increased model utility. For DP-SGD, there already exist solutions to achieve personalized DP by tracking DP costs individually, per data point, and removing data from training whose budget is exhausted [13]. However, to the best of our knowledge, no such approaches for the PATE-framework have been proposed, so far, and the existing methods for DP-SGD cannot be applied to PATE. Supporting personalized privacy also in PATE is of high relevance though, since PATE supports a wide range of scenarios in which DP-SGD is not that easily applicable: While DP-SGD is mainly applicable in centralized learning applications with a non-convex model architecture, PATE can also be applied to distributed learning scenarios even when different participants hold different types of models with different training algorithms and architectures. Additionally, since in DP-SGD, privacy bounds dependent on the model parameters, for large models, the privacy guarantees will degrade which is not the case for PATE [12].

In this work, we, therefore, propose three novel PATE variants namely *upsampling*, *vanishing*, and *weighting* which are able to make use of personalized privacy budgets among the data points. We first define them theoretically and provide a detailed privacy analysis. Then, we experimentally evaluate their implications on the resulting model utility for the MNIST [14] and Adult income [15] datasets and investigate how different distributions of privacy budgets influence the gained utility. Our experiments show that in comparison to the original PATE approach in which the privacy budget of the entire dataset is determined by the data point with the highest privacy requirements, our personalized PATE variants generate significantly more labels. Depending on the privacy budget distribution and the PATE variant, we are able to produce approximately between +60% to +950% more labels for the MNIST, and +60% to +890% for the Adult income dataset. The contribution of this work can be summarized as follows:

- Introduction of three novel personalized PATE variants;
- Theoretical analysis of the respective privacy bounds;
- Experimental evaluation of utility improvements for the MNIST and Adult income dataset;
- Quantification of the effects of different privacy budget distributions on the gained utility;

For the experiments, we used the Confident-GNMax algorithm [16], *i.e.*, privacy protection is ensured by Gaussian noise within PATE and labels are only produced if a consensus among the teachers is reached. Additionally, we do neither perform virtual adversarial training [17] nor MixMatch [18], both semi-supervised techniques shown to improve the accuracy of the model to be published for PATE.

**Ethical Implications and Impact of our Work** In general, deciding on an adequate privacy budget  $\epsilon$  in ML applications with DP on sensitive data is a challenging task since the real-world implications of concrete values for  $\epsilon$  are poorly understood. Additionally, even the calculated privacy budgets  $\epsilon$  for the same application and data might decrease over time, when tighter bounds for their calculation are pushed forward [19]. These inherent problems of DP in ML are also faced when assigning individual privacy budgets to data points. In particular, one needs to make sure that no entity training an ML model with individual DP guarantees abuses their power and assigns poor levels of privacy to individual data that actually needs it. We therefore, suggest the use of our new personalized PATE variants in settings that contain a process for obtaining informed consent of the data holders to process their data at a given privacy level, such as [20]. This process should consist of (1) the identification of the individual privacy preferences [21, 22], (2) the communication of the privacy risks and limitations of data use through transparency (*e.g.* [23]), and (3) enabling meaningful decision-making processes by providing information about DP concerning sensitive data disclosure (*e.g.* [24]). Moreover, we argue that, due to its difficult interpretability, individual data holders should not be in charge of choosing their numeric privacy budget  $\epsilon$ , but, based on the information on potential risks and benefits decide on an abstract privacy level, such as "low", "medium", or "high" [25]. Concrete numeric values  $\epsilon$  could then be fixed by the regulator or ethics committee in charge depending on the sensitive data itself and the application [26].

## 2 Background & Notation

This section provides the theoretical foundation of the work at hand and introduces the notation used throughout the paper.

### 2.1 Notation

We call  $\mathcal{D}$  and  $\mathcal{R}$  the sets of all possible data points, and all possible processing results that can be produced on them, respectively. Furthermore, two concrete datasets  $D, D' \subseteq \mathcal{D}$  are called neighboring (written  $D \sim D'$ ) if  $D$  and  $D'$

differentiate exactly in one data point. More specifically, they are called neighboring on  $d$  (written  $D \stackrel{d}{\sim} D'$ ) if they differentiate exactly in the data point  $d \in \mathcal{D}$ .

To refer to  $\varepsilon$ , we will use the term *privacy budget* when expressing the privacy preference specified before the analysis, and the term *privacy costs* when referring to the proportion of budget being already consumed in a DP-based mechanism.

All log values in this work are based on the natural logarithm. Furthermore,  $\mathbb{P}[\cdot]$  denotes the probability of an event according to an adequate probability measure, and  $\mathbb{E}[\cdot]$  outputs the expected value of a given random variable.

## 2.2 Differential Privacy

DP formalizes the idea of limiting the influence of individual data points on results of analyses conducted on a whole dataset. One relaxation of the standard definition of DP is called  $(\varepsilon, \delta)$ -DP.

**Definition 1** (cf. [27], Def. 2.4). Let  $D, D' \subseteq \mathcal{D}$  be two neighboring datasets (written  $D \sim D'$ ), i.e. two datasets that differ in at most one data point. Let  $M: \mathcal{D}^* \rightarrow \mathcal{R}$  be a mechanism that processes arbitrarily many data points.  $M$  satisfies  $(\varepsilon, \delta)$ -DP with  $\varepsilon \in \mathbb{R}_+$  and  $\delta \in [0, 1]$  if for all datasets  $D \sim D'$ , and for all result events  $R \subseteq \mathcal{R}$

$$\mathbb{P}[M(D) \in R] \leq e^\varepsilon \cdot \mathbb{P}[M(D') \in R] + \delta. \quad (1)$$

Thereby, it expresses the guarantee that a single data point cannot alter the probability of any processing result by a factor larger than  $\exp(\varepsilon)$  or smaller than  $1/\exp(\varepsilon)$ . The second parameter  $\delta$  specifies a small density of probability on which the upper bound does not have to hold.

In ML, data are usually processed multiple times to train a model, e.g. by conducting several training epochs. This process can be considered as a *composition* of mechanisms that each have privacy costs. The following composition theorem states how DP behaves under composition as follows.

**Proposition 1** (cf. [28], Thm. 3.16). Let  $\mathcal{R}_1, \mathcal{R}_2$  be two arbitrary result spaces. Let further  $M_1: \mathcal{D}^* \rightarrow \mathcal{R}_1$ ,  $M_2: \mathcal{D}^* \rightarrow \mathcal{R}_2$  be mechanisms that satisfy  $(\varepsilon_1, \delta_1)$ - and  $(\varepsilon_2, \delta_2)$ -DP, respectively. Then, the composition  $M_3(D) \mapsto (M_1(D), M_2(D))$  satisfies  $(\varepsilon_1 + \varepsilon_2, \delta_1 + \delta_2)$ -DP.

The proof can be found in Appendix B of [28].

## 2.3 Rényi Differential Privacy

Proposition 1 shows that under composition,  $(\varepsilon, \delta)$ -DP quickly leads to a combinatorial explosion of parameters. A smoother composition of privacy bounds can be achieved by using Rényi Differential Privacy (RDP) [29] that is based on the Rényi divergence (see Definition 10 in Appendix A).

**Definition 2** (cf. [29], Def. 4). A mechanism  $M: \mathcal{D}^* \rightarrow \mathcal{R}$  satisfies  $(\alpha, \varepsilon)$ -RDP with  $\alpha \in \mathbb{R}_+ \setminus \{1\}$  and  $\varepsilon \in \mathbb{R}_+$  if for all datasets  $D \sim D'$  and for all result events  $R \subseteq \mathcal{R}$

$$\mathbb{D}_\alpha [f_{M(D)} \parallel f_{M(D')}] \leq \varepsilon. \quad (2)$$

Here,  $f_{M(D)}$  and  $f_{M(D')}$  are the probability distributions of the results of  $M$  on  $D$  and  $D'$ , respectively.

In Lemma 3, and Lemma 4 in the Appendix A, we show the composition and transformation from RDP to DP guarantees, respectively.

## 2.4 Personalized Differential Privacy

Personalized DP, such as proposed in [30, 31, 32, 33], allows to account privacy for data points individually.

**Definition 3** (cf. [30], Def. 6). For any data point  $d \in \mathcal{D}$ ,  $M$  satisfies  $(\varepsilon_d, \delta_d)$ -DP with  $\varepsilon_d \in \mathbb{R}_+$  and  $\delta_d \in [0, 1]$  if for all datasets  $D \stackrel{d}{\sim} D'$ , and for all result events  $R \subseteq \mathcal{R}$

$$\mathbb{P}[M(D) \in R] \leq e^{\varepsilon_d} \cdot \mathbb{P}[M(D') \in R] + \delta_d. \quad (3)$$

The idea of accounting privacy per data point can also be applied to different DP variants, such as RDP. Thereby, DP properties like composition and transformation apply analogously to the original concepts.

## 2.5 PATE

The PATE framework [12] can be used to perform supervised ML with DP guarantees. Therefore, the set of private labeled training data is split among a pre-defined number of so-called *teacher* models and each teacher is trained on their partition of the data. Afterwards, the knowledge gained by the teachers from the private training data is transferred to a public so-called *student* model. To do so, the teachers label a public and unlabeled dataset as training data for the student. Privacy protection for the teachers' sensitive training data is obtained by adding DP noise in that labeling process, and by the fact that the student does not get to interact with the sensitive data, but instead uses the public dataset for training. See Figure 1a for an overview on the approach.

The DP noise addition in the labeling process determines the privacy level of the PATE algorithm. To obtain a label for a public data point, each teacher issues a vote for a specific class, and these votes are aggregated with the Gaussian NoisyMax Aggregator as follows:

**Definition 4** (cf. [12], Sec. 2.1). Let  $\mathcal{X}, \mathcal{Y}$  be the feature space, and the set of classes corresponding to a data distribution, respectively. Further, let  $t_i: \mathcal{X} \rightarrow \mathcal{Y}$  be the  $i$ -th teacher of a teacher ensemble of size  $k \in \mathbb{N}$ . The vote count  $n: \mathcal{Y} \times \mathcal{X} \rightarrow \mathbb{N}$  of any class  $j \in \mathcal{Y}$  for any data point  $x \in \mathcal{X}$  is

$$n_j(x) := \sum_{i=1}^k \mathbb{1}(t_i(x) = j) . \quad (4)$$

The characteristic function  $\mathbb{1}: \{\perp, \top\} \rightarrow \{0, 1\}$  maps 'true' to 1 and 'false' to 0. Note that the vote count depends on the teachers and therefore also on their training data.

**Definition 5** (cf. [16], Sec. 4.1). Let  $n_j$  be the vote count as defined in Definition 4 for each class  $j \in \mathcal{Y}$ . Then, the Gaussian NoisyMax (GNMax) aggregation method with parameter  $\sigma \in \mathbb{R}_+$  on any data point  $x \in \mathcal{X}$  is given by

$$\text{GNMax}_\sigma(x) := \arg \max_{j \in \mathcal{Y}} \{n_j(x) + \mathcal{N}(0, \sigma^2)\} . \quad (5)$$

The Gaussian noise is sampled from a normal distribution  $\mathcal{N}(\mu, \sigma^2)$  with mean  $\mu = 0$  and variance  $\sigma^2$ .

As an extension of the original GNMax Aggregator, Papernot *et al.* [16] proposed the *Confident-GNMax Aggregator* that only labels data points for which the consensus of the teachers exceeds a pre-defined threshold. See [16] for a formalization of this idea.

## 3 Personalized Extensions for PATE

In order to implement individual privacy requirements of sensitive training data points, in this section, we propose three novel aggregation mechanisms for PATE based on the original GNMax Aggregator, namely the *upsampling*, *vanishing*, and *weighting*-mechanism. Each variant deviates from the original PATE assumptions in some aspects in order to provide personalized privacy. If all sensitive data points require the same privacy, the personalized PATE variants are equal to non-personalized PATE.

In this section, we first introduce the ideas behind all three mechanisms and then perform an evaluation of their privacy levels. Therefore, we rely on the privacy analysis of the original PATE algorithm [12], and extend it to our individual variants by analyzing the sensitivity of the vote counts.

### 3.1 Upsampling-Mechanism

Our first approach that we call *upsampling* (see Figure 1b) relies on duplicating sensitive data such that overlapping data subsets are allocated to the different teachers. This idea stands in contrast to the original PATE algorithm where disjoint data partitions are passed to the teachers. Through the upsampling approach, data with higher privacy budgets will be learned by a higher number of teachers. The duplicates extend the amount of training data such that either more data is available per teacher or that a larger number of teachers can be trained. We call the aggregator based on this approach and Gaussian noise *upsampling GNMax (uGNMax)*. It applies the *upsampling vote count* which is defined as follows.

**Definition 6** (Upsampling Vote Count). Let  $t_i: \mathcal{X} \rightarrow \mathcal{Y}$  be the  $i$ -th out of  $k \in \mathbb{N}$  teachers. Let further  $N \in \mathbb{N}$  be the number of sensitive data points and  $m_i \in \{0, 1\}^N$  a mapping that describes which points are learned by  $t_i$ . The upsampling vote count  $\tilde{n}: \mathcal{Y} \times \mathcal{X} \rightarrow \mathbb{N}$  of any class  $j \in \mathcal{Y}$  for any data point  $x \in \mathcal{X}$  is

$$\tilde{n}_j(x) := \sum_{i=1}^k \mathbb{1}(t_i(x) = j) . \quad (6)$$

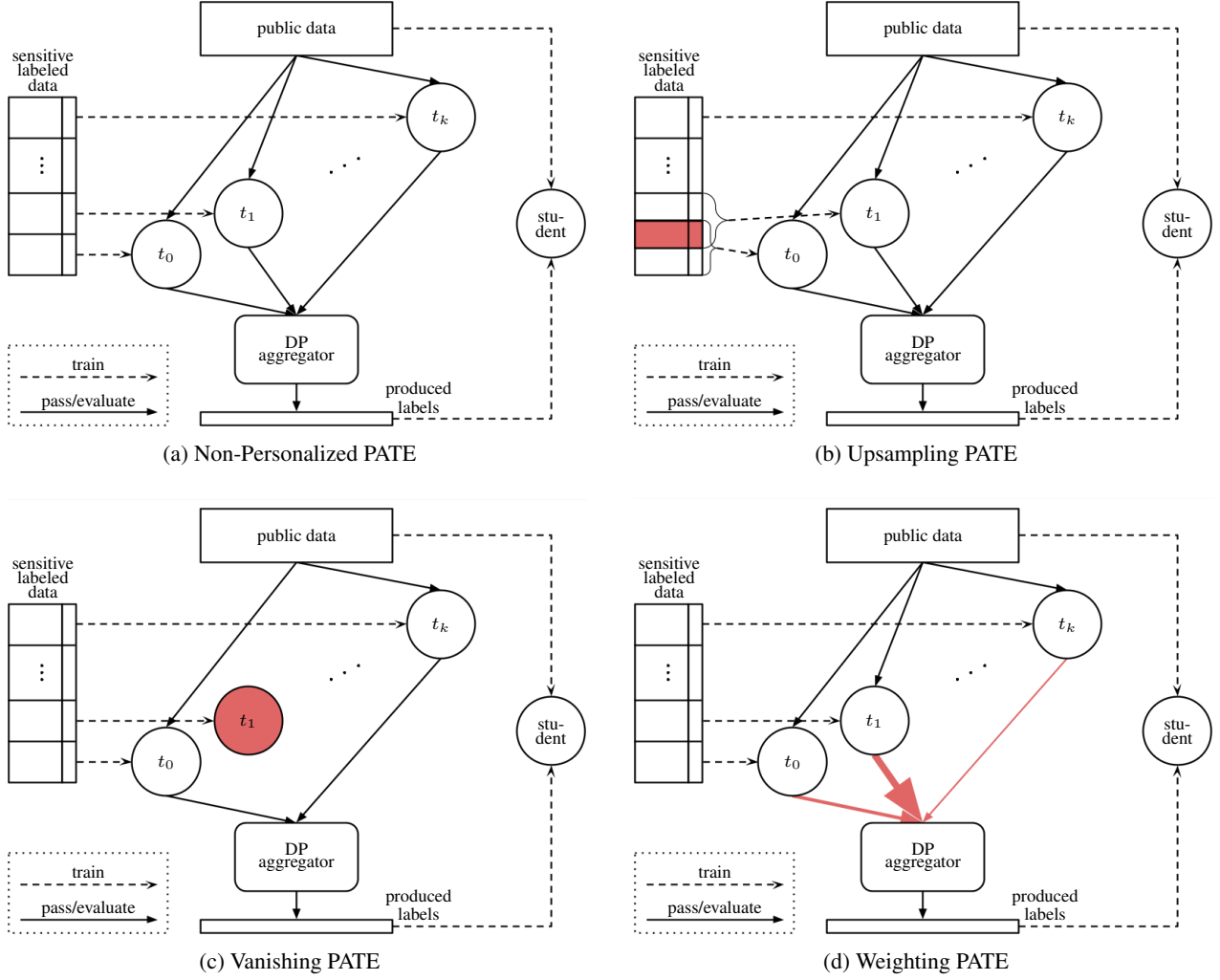


Figure 1: **PATE Schemes.** Teachers  $t_0, t_1, \dots, t_k$  are trained on partitions of sensitive labeled data. Afterwards, public unlabeled data is given to the teacher ensemble whose votes are aggregated *s.t.* labels are produced. Finally, the student is trained on the public data with produced labels. The personalized variants modify this procedure to individually adjust the influence of sensitive data on produced labels. Sensitive data may be used to train multiple teachers (b). Instead, teachers may avoid participating in some votings (c), or be weighted differently (d).

Note that, although the definition for the upsampling vote count looks the same as the non-personalized vote count (Definition 4), their sensitivities differ due to data points to be learned by several teachers (see Proposition 2 in Section 3.4.2).

### 3.2 Vanishing-Mechanism

Our second mechanism that we call *vanishing* (see Figure 1c) keeps the independent partitioning of the original PATE approach and asserts personalized privacy budgets by having teachers participate in more or less votings. Therefore, data points with the same privacy budgets need to be allocated to the same teacher(s), such that teachers that contain data points with higher privacy requirements (lower budgets) can contribute in less votings. We call the resulting aggregation method *vanishing GMax* (*vGMax*). Its vote count mechanism can be defined as follows.

**Definition 7** (Vanishing Vote Count). Let  $t_i: \mathcal{X} \rightarrow \mathcal{Y}$  be the  $i$ -th out of  $k \in \mathbb{N}$  teachers. Let further  $N \in \mathbb{N}$  be the number of sensitive data points and  $m_i \in \{0, 1\}^N$  a mapping that describes which points are learned by  $t_i$ . Moreover, let  $s_i \in \{0, 1\}$  be the current participation of  $t_i$ . The vanishing vote count  $\hat{n}: \mathcal{Y} \times \mathcal{X} \rightarrow \mathbb{N}$  of any class  $j \in \mathcal{Y}$  for any

unlabeled public data point  $x \in \mathcal{X}$  is defined as

$$\hat{n}_j(x) := \sum_{i=1}^k s_i \cdot \mathbb{1}(t_i(x) = j) . \quad (7)$$

### 3.3 Weighting-Mechanism

Our third approach that we call *weighting* (see Figure 1d) is similar to vanishing PATE in the sense that it also scales the influence of individual teachers differently. However, in the weighting approach each teacher always participates in the voting process and scaling is implemented by assigning specific weights to each teacher’s votes. Therefore, similar to the vanishing approach, sensitive data with same privacy budgets have to be allocated to the same teacher(s). We call the aggregation method of this PATE variant *weighting GNMax (wGNMax)*. Its vote count mechanism is defined in Definition 8.

**Definition 8** (Weighting Vote Count). Let  $t_i: \mathcal{X} \rightarrow \mathcal{Y}$  be the  $i$ -th out of  $k \in \mathbb{N}$  teachers. Let further  $N \in \mathbb{N}$  be the number of sensitive data points and  $m_i \in \{0, 1\}^N$  a mapping that describes which points are learned by  $t_i$ . Moreover, let  $\psi_i \in \mathbb{R}_+$  be the weight of  $t_i$  for all  $i \in \{1, \dots, k\}$ . The weighting vote count  $\tilde{n}: \mathcal{Y} \times \mathcal{X} \rightarrow \mathbb{N}$  of any class  $j \in \mathcal{Y}$  for any unlabeled public data point  $x \in \mathcal{X}$  is

$$\tilde{n}_j(x) := \sum_{i=1}^k \psi_i \cdot \mathbb{1}(t_i(x) = j) . \quad (8)$$

### 3.4 Privacy Evaluation

The privacy calculation of personalized PATE differs from non-personalized PATE in that it is done for particular data points or groups of data points separately, rather than for the whole dataset. In this section, we first introduce the general elements of the privacy analysis in non-personalized PATE which is shared by all our three approaches. Then, we evaluate the personalized privacy guarantees of each approach dependent on its vote count and aggregation mechanism.

#### 3.4.1 Privacy Evaluation of Non-Personalized PATE

A key element of privacy calculation in PATE is the aggregation mechanism. PATE’s GNMax Aggregator mechanism is a function of a Gaussian mechanism.

**Definition 9** (cf. [28], Sec. 3.5.3). Let  $f: \mathcal{D}^* \rightarrow \mathbb{R}^z$  with  $z \in \mathbb{N}$  be any real-valued function and let  $\sigma \in \mathbb{R}_+$  be any positive real. Then, the Gaussian mechanism of  $f$  with standard deviation  $\sigma$  is

$$M_{f,\sigma}(x) := f(x) + \mathcal{N}(0, \sigma^2) . \quad (9)$$

Note that the same random noise value is added to  $f(x)$  in each dimension.

Gaussian mechanisms have RDP costs depending on  $\sigma$ .

**Lemma 1** (cf. [29], Prop. 7). Let  $\sigma \in \mathbb{R}_+$  and let  $f: \mathcal{D}^* \rightarrow \mathbb{R}$  be a real-valued function with sensitivity  $\Delta_f := \max_{D \sim D'} \|f(D) - f(D')\|_2$ . Then, the Gaussian mechanism  $M_{f,\sigma}$  satisfies  $(\alpha, \Delta_f^2 \cdot \alpha/2\sigma^2)$ -RDP for all  $\alpha \in \mathbb{R}_+ \setminus \{1\}$ .

Lemma 1 is proven in [29]. The resulting RDP costs can be transformed into  $(\epsilon, \delta)$ -DP costs using Lemma 4.

A rough estimate of the privacy costs that arise in PATE can be given by the data-independent *loose bound*.

**Lemma 2** (cf. [16], Prop. 8). The GNMax aggregator satisfies  $(\alpha, \alpha/\sigma^2)$ -RDP for all  $\alpha \in \mathbb{R}_+ \setminus \{1\}$ .

The intuition behind it is that in PATE, each data point of the training dataset is learned by exactly one teacher and might be able to completely change this teacher’s vote. Since DP guarantees are expressed for neighboring datasets that differ in exactly one data point  $d$ , in the worst case,  $d$  changes the vote count for two classes (reduce one class count by one, and increase another class count by one). Thus, a teacher voting can be considered as the composition of two Gaussian mechanisms each with sensitivity  $\Delta_f = 1$  and parameter  $\sigma$  equal to the standard deviation of the Gaussian noise. Putting the standard deviation of one into Lemma 1, and applying composition of two Gaussian mechanisms, this yields the term specified in the loose bound.

In addition, it is also possible to obtain a tighter data-dependent bound for privacy estimation in PATE as defined in [16]. See Lemma 5 in Appendix A for a definition of this *tight bound*.

### 3.4.2 Personalized Privacy Evaluation of PATE

All our new aggregation mechanisms apply personalized vote counts  $\bar{n}: \mathcal{Y} \times \mathcal{X} \rightarrow \mathbb{N}$  whose sensitivities are no longer  $\Delta_f = 1$ , but are determined individually for particular data points (or groups of data points). Therefore, in the privacy analysis, we need to calculate their privacy bounds based on the mechanisms' individual sensitivities and the general privacy bounds of PATE.

The individual sensitivity of any function  $f: \mathcal{D}^* \rightarrow \mathbb{R}^z$  with  $z \in \mathbb{N}$  regarding any data point  $d \in \mathcal{D}$  can be defined as  $\Delta_{f,d} := \max_{D \stackrel{\mathcal{L}}{\sim} D'} \|f(D) - f(D')\|_2$ . The following three propositions formalize the individual sensitivity of the vote counts in our personalized PATE mechanisms.

**Proposition 2** (Upsampling Sensitivity). *Let  $d \in \mathcal{D}$  be any sensitive data point. Let  $u_d \in \mathbb{N}$  be the number of duplicates of  $d$  (incl. the original  $d$ ). Then, the individual sensitivity of the vote count, regarding  $d$ , in upsampling PATE is*

$$\Delta_{\text{upsampling},d} = u_d. \quad (10)$$

*Proof.* In upsampling PATE, every teacher that was trained on data point  $d \in \mathcal{D}$  can have a different vote for neighboring datasets that differ in  $d$ . For each duplicate of  $d$ , this results in an increase of one vote count and a decrease of another one. Let  $t_{(d)}$  be the set of teachers trained on  $d$ . Assume that all  $u_d$  votes of  $t_{(d)}$  would have changed if  $d$  were different. From the perspective of  $d$ , the voting can then be considered as a composition of  $2 \cdot |\mathcal{Y}|$  Gaussian mechanisms (some might have a sensitivity of zero *s.t.* they have no privacy costs). For each class  $j \in \mathcal{Y}$  there are two Gaussian mechanisms, one with sensitivity equal to the number of votes of  $t_{(d)}$  for  $j$  if  $d$  were changed, the other if  $d$  were not changed. Applying Lemma 2 and Lemma 3 yields a sum of RDP values, each dependent on its specific sensitivity. Since the sensitivity has a quadratic impact on the RDP costs of a Gaussian mechanism, votes for the same class are more expensive than votes for different classes. Therefore, the RDP costs are the highest if all  $u_d$  teachers trained on  $d$  would consent on a class  $j$  when trained on  $d$  and would consent on class  $j' \neq j$  if  $d$  would be different.  $\square$

**Proposition 3** (Vanishing Sensitivity). *Let  $d^{(i)} \in \mathcal{D}$  be a sensitive data point learned by teacher  $t_i \in \{t_1, \dots, t_k\}$ . Let  $s := (s_1, \dots, s_k) \in \{0, 1\}^k$  be the selection to determine which teachers participate in the current voting. Then, the individual sensitivity of the vanishing vote count, regarding  $d^{(i)}$ , is*

$$\Delta_{\text{vanishing},d}^{(i)} = s_i. \quad (11)$$

*Proof.* In vanishing PATE, every data point only influences the vote of one teacher, which, in the worst case results in two vote counts being changed. However, in contrast to non-personalized PATE, privacy is only spent if the teacher corresponding to  $d^{(i)}$  participates in the current voting.  $\square$

**Proposition 4** (Weighting Sensitivity). *Let  $d^{(i)} \in \mathcal{D}$  be a sensitive data point learned by teacher  $t_i \in \{t_1, \dots, t_k\}$ . Let  $w_i$  be the weight to determine the influence of  $t_i$  to votings. Then, the individual sensitivity of the weighting vote count, regarding  $d^{(i)}$ , is*

$$\Delta_{\text{weighting},d}^{(i)} = w_i. \quad (12)$$

*Proof.* In weighting PATE, every data point only influences one teacher. Therefore, on neighboring datasets, every vote count might change by the corresponding teacher's weight  $w_i$ .  $\square$

Based on the mechanisms' sensitivity, we can formulate the loose bound of our personalized aggregation mechanisms as follows:

**Theorem 1** (Individual Loose Bound). *Let  $M$  be a personalized GNMax aggregator with noise scale  $\sigma \in \mathbb{R}_+$ . Let further  $d \in \mathcal{D}$  be any data point, and  $\Delta_{M,d}$  be the individual sensitivity of  $M$ 's personalized vote count regarding  $d$ . Then,  $M$  satisfies an individual  $(\alpha, (\Delta_{M,d})^2 \cdot \alpha/\sigma^2)$ -RDP regarding  $d$  for all  $\alpha \in \mathbb{R}_+ \setminus \{1\}$ .*

*Proof.* Personalized GNMax aggregators can be considered as the composition of all classes' vote counts regarding each data point. Only two<sup>1</sup> of them can be changed at the same time on neighboring datasets. Thus, the two Gaussian mechanisms with an individual sensitivity per data point are composed. Therefore, the claimed RDP guarantee is achieved by using Lemma 1 on privacy guarantees of Gaussian mechanisms, and Lemma 3 from Appendix A on composition.  $\square$

<sup>1</sup>In the upsampling approach, more than two vote counts can be changed. But the worst case is if all teachers affected by the same point change the same vote counts (see the proof of Proposition 2).

As for the non-personalized GNMax aggregator, the data-dependent tight bound (see Lemma 5 in Appendix A) can be applied to the personalized GNMax aggregators where all data sharing the same individual sensitivity also share the same tight bound. The tight bound builds up on the loose bound and assumes a sensitivity equal to one. Since sensitivity and noise scale are invariantly related to each other as the following corollary indicates, the tight bound can be applied using the noise scale relative to the individual sensitivity *s.t.* the latter equals one.

**Corollary 1** (Scaling Invariance of the Individual Loose Bound). *Let  $c \in \mathbb{R}_+$  be any positive scalar. Let  $M$  be a personalized GNMax aggregator with noise scale  $\sigma \in \mathbb{R}_+$  and an individual sensitivity  $\Delta_{M,d} \in \mathbb{R}_+$  for some data point  $d \in \mathcal{D}$ . Furthermore, let  $\tilde{M}$  be another personalized GNMax aggregator with noise scale  $\tilde{\sigma} = c \cdot \sigma$  and individual sensitivity  $\Delta_{\tilde{M},d} = c \cdot \Delta_{M,d}$  regarding  $d$ . Then,  $M$  and  $\tilde{M}$  have the same individual loose bound regarding  $d$  for any  $\alpha \in \mathbb{R}_+ \setminus \{1\}$ .*

*Proof.* Fix  $\alpha \in \mathbb{R}_+ \setminus \{1\}$ .  $M, \tilde{M}$  satisfy individual  $(\alpha, \varepsilon)$ - and  $(\alpha, \tilde{\varepsilon})$ -RDP, respectively, regarding  $d$ . The equality of  $\varepsilon$  and  $\tilde{\varepsilon}$  is verified by direct computation as follows.

$$\begin{aligned}
 \tilde{\varepsilon} &:= \left( \Delta_{\tilde{M},d} \right)^2 \cdot \alpha / \tilde{\sigma}^2 \\
 &= (c \cdot \Delta_{M,d})^2 \cdot \alpha / (c \cdot \sigma)^2 \\
 &= c^2 \cdot (\Delta_{M,d})^2 \cdot \alpha / c^2 \cdot \sigma^2 \\
 &= (\Delta_{M,d})^2 \cdot \alpha / \sigma^2 \\
 &=: \varepsilon
 \end{aligned} \tag{13}$$

□

## 4 Experimental Setup

This section describes implementation details of our proposed approaches as well as insights on the experiments conducted to empirically evaluate them.

### 4.1 Framework

We created a framework that comprises Gaussian PATE (GNMax, Confident-GNMax, Interactive-GNMax), our proposed personalized variants, and the support for experimentation. Except for the tight bound and corresponding helper functions which were taken from [34], the whole framework was implemented from scratch using Python [35] (version 3.8).

### 4.2 Datasets and Models

We conducted our experiments on two different datasets, namely MNIST [14] and the Adult income dataset [15]. The former one consists of 70,000 ( $28 \times 28$ )-pixel gray-scale images depicting handwritten digits for classification. We scaled the pixel values of all images to the range of zero to one. The latter Adult income dataset contains 48,842 tabular data points from the US census of the year 1994. The corresponding classification task is to predict if the yearly income of a person represented in the data is greater than \$50k. As a pre-processing of the data, we removed 3,620 damaged data points from the dataset and transformed categorical features into numerical values. Furthermore, we normalized these numerical values to the range of zero to one.

To train the teacher and student models on MNIST, we used a simple convolutional neural network (CNN) architecture taken from [36] (see Table 1). All weights in the output layer were initialized by values randomly sampled from the Glorot uniform distribution, whereas all other weights were sampled from the He uniform distribution. Optimization was performed using the Adam optimizer and categorical cross-entropy loss. All other parameters were set according to the default values from TensorFlow (version 2.4.1).

For the Adult income dataset, the teacher and student models were implemented by random forest models from the scikit-learn library. Each random forest consisted of 100 decision trees. Otherwise, the default parameters of the library were kept.

Since every teacher only got about 240 data points for training in the MNIST experiments, we applied a custom data augmentation within each individual teacher and the student to improve model performances. So, each data point within one model’s training data was randomly rotated by up to  $\pm 7.5^\circ$  and randomly shifted by up to 7% both, in horizontal



layer	type of layer	parameters	activation
1	convolutional	32 (3, 3)-kernels	ReLU
2	batch normalization	-	-
3	max pooling	size (2, 2)	-
4	flatten	-	-
5	fully connected	100 nodes	ReLU
6	batch normalization	-	-
7	fully connected	10 nodes	softmax

Table 1: CNN-architecture for MNIST.

and vertical direction to make a larger training dataset for that model. This data augmentation does not influence the privacy costs since we augment the data points only within a model’s training dataset and not over different datasets. Therefore, augmented data points will be used to train the same model as their original data points, and PATE is already based on the assumption that each single data point could completely determine the behavior of a corresponding teacher model (*cf.* Lemma 2 and Lemma 5). Hence each data point can be augmented and duplicated without additional DP costs. For the experiments based on the Adult income data, no data augmentation was applied since it did not yield performance benefits.

### 4.3 Evaluation Metrics

To measure utility of the different PATE variants and privacy budget distributions, we tracked two metrics. First, we counted the *number of produced labels* until any of the specified privacy budgets was exhausted. Second, we measured the *accuracy* of the student model trained on that resulting labeled data.

As baselines to compare our methods to, we conducted experiments with non-personalized Confident-GNMax using the *minimum*, *maximum*, or *average* budget of a corresponding personalized experiment. Since, also for non-personalized PATE, no data point’s privacy requirement shall be violated, the minimum baseline is the most important one. The maximum and average baselines constitute the cases of all sensitive data having the maximum or the average budget among individual privacy budgets in personalized experiments and thereby provide natural reference values.

### 4.4 PATE Experiments

To experimentally evaluate our three novel personalized PATE variants, we conducted experiments in four steps. (1) At first, the complete dataset was randomly divided into a private, public, and test partition. The sizes of these partitions as well as general parameters for Confident-GNMax and its personalized variants on both datasets are described in Table 2. Nevertheless, the parameters were adapted in the upsampling and the vanishing approach so that teacher accuracies and voting accuracies align with those of weighting and non-personalized experiments. (2) Privacy budgets were randomly assigned to the private data according to a given privacy budget distribution. Afterwards, the data was allocated to the corresponding teacher models for training. (3) The trained teachers were used to produce labels in a voting process. Aggregation of the teacher votes was conducted according to the PATE variant under evaluation. As a baseline to evaluate our three variants, we used the original non-personalized Confident-GNMax. After every voting, the current accumulated RDP costs of data points were computed and stored group-wise<sup>2</sup> for all natural RDP  $\alpha$  values from two to 50. Thereafter, these RDP costs were transformed into standard DP costs by taking the best  $\alpha$  at that point of the voting as RDP order. After 2,000 produced labels, the voting process was terminated since we observed that all experiments could exhaust their privacy budget within that number. Tracking privacy costs above the actual budget exhaustion up to the fixed number of 2,000 generated labels was done to compare the cost histories of different experiments over many votings. (4) The student model was trained on the labeled data that the respective teacher ensemble produced until any private data point’s privacy budget was exceeded. In order to get more reliable results, we averaged our measurements in all following experiments over multiple runs—that is ten teacher ensembles each with five voting processes—for the same parameters with different random initialization for data shuffling and noise invoked.

#### 4.4.1 Aligning Privacy Budgets and Costs

We showed how the parameters (numbers of duplications for upsampling, participation frequencies for vanishing, and teacher weights for weighting) for personalized PATE influence the individual loose bound through individual

<sup>2</sup>For *upsampling*, all data points that share the same number of duplicates have the same privacy costs. In the *vanishing* approach, all data points within the same teacher have the same privacy costs. For *weighting*, all data points that were learned by teachers of the same weight exhibit the same privacy costs.

dataset	# teachers	# data	private	public	test	$\sigma_1$	$\sigma_2$	$T$	$\delta$
MNIST	250		60,000	9,000	1,000	150	40	200	$10^{-5}$
Adult	250		37,222	7,000	1,000	200	40	300	$10^{-5}$

Table 2: **PATE Parameters.** Parameters used in the experiments for the Confident-GNMax on the MNIST and Adult income datasets.  $\sigma_2$  is the standard deviation of noise induced to the label aggregation.  $\sigma_1$  specifies the standard deviation of noise used to check if the teachers have a consensus together with the threshold  $T$ .

sensitivities. But the actual privacy costs depend not only on the loose bound but instead on the data-dependent tight bound and on the currently optimal RDP order(s). Therefore, it does not suffice to set the individual parameters or sensitivities proportional to the individual budgets.

To find adequate parameters, we first conducted experiments to analyze the relation between individual sensitivities and resulting privacy costs. The goal was to relate individual sensitivities by adjusting parameters so that all privacy budgets exhaust approximately at the same time. To enable comparisons among the different variants, we described the parameters by corresponding individual sensitivities. We randomly divided the sensitive data into two equally sized groups, one with higher and one with lower individual sensitivity. The parameters were adjusted so that a ratio of  $c \mid 1$  was achieved for individual sensitivities with each  $c \in \{2, \dots, 9\}$ . We conducted this experiment on the MNIST dataset and trained ten different ensembles. Each ensemble was then used for five different voting processes. We performed 4,000 votings in each process to compare the different cost growths over time.

#### 4.4.2 Random Assignment of Privacy Budget

We conducted our first set of experiments on both datasets with various privacy budget distributions. For simplicity, we assigned one of two different budgets (a higher and a lower budget) to every data point in the private dataset randomly. We varied the ratio of data points having the higher budget among 25%, 50%, and 75%. The lower budget was set to  $\log 2 \approx 0.69$  over all experiments while we assigned the higher budget from  $\log 4$ ,  $\log 8$ , and  $\log 16$ .

Using logarithmic values provides more intuitive comparison among the privacy budgets since the formulation of DP (Definition 1) uses  $\exp(\varepsilon)$ . Hence, an  $\varepsilon = \log s$  for any real  $s \geq 1$  is half of a privacy budget  $\varepsilon' = \log 2s$ . For example with our chosen budgets, a budget of  $\varepsilon = \log 8$  is four times as high as a budget of  $\varepsilon' = \log 2$ . The data and resulting labels that were produced until any data point’s privacy budget was exhausted were used to train the student models.

#### 4.4.3 Class-Dependent Assignment of the Privacy Budget

PATE, similar to many ML algorithms, in particular when DP is involved [37], has more difficulties learning data at tails of the distribution, *i.e.* outliers. Knowledge about data with rare properties can be lost in two ways. (1) Teachers that are trained on too few data points that share a specific property may not gain knowledge about it. (2) If the majority of teachers has no knowledge about the outliers, even if a minority of teachers has, in the voting process, the information about them can not be passed to the produced labels. In some cases, an underrepresentation of data can be compensated by duplicating them, for example through the upsampling PATE variant. Note, however, that duplication increases the individual privacy costs of the original data point.

The Adult income dataset’s class distribution is skewed (incomes lower than \$50k make 75.2% of the dataset). This might reflect in reduced classification performance. In our second set of experiments, we, therefore, set out to investigate whether performance of the PATE algorithm could be improved by increasing the privacy budget for only small parts of the data—if that data is expressive, *i.e.* from the underrepresented class. If so, larger parts of the data could be awarded high privacy protection, while achieving improved model utility.

In contrast to the previously described experiments, only the upsampling approach was used for the experiments here. This is due to the fact that for vanishing and weighting PATE, only data points with the same budget are given to the same teacher(s). But then, either the teachers are exclusively trained on points of the same class or those of the more frequent class need to have the higher budget as well. In the first case, teachers would perform very badly while the second case would not fit our intended analysis.

We set the higher budgets again to  $\log 4$ ,  $\log 8$ , and  $\log 16$  during our experiments, and kept the lower budget at  $\log 2$ . Additionally, we varied the ratio of data in the underrepresented class that would receive the higher privacy budget among 25%, 50%, 75%, and 100%. For each budget and ratio combination, we again trained ten teacher ensembles for each personalized GNMax variant and used them for five voting processes each. The data and corresponding labels that were produced until any data point’s privacy budget was exceeded were then used to train the student models.

## 5 Results

This section presents the results of our experiments described in the previous section. We first depict how to set the parameters of the personalized variants so that different privacy budgets are exhausted at approximately the same time. Then, we show the quantitative effects of personalization in PATE based on the metrics from Section 4.3.

### 5.1 Setting Parameters for Personalized Variants

Figure 4 in Appendix C visualizes the relation between the parameters of our personalized Confident-GNMax variants and the resulting personalized privacy costs according to tight bounds over time. We observe that uGNMax and wGNMax behave very similarly and their cost ratios stay almost constant after a few votings. Contrary, vGNMax needs more votings to lower the gain of its cost ratio. For uGNMax and wGNMax, the cost ratio according to the tight bound seems to be approximately equal to the ratio of sensitivities, whereas the cost ratio approaches the square root of the ratio of sensitivities for vGNMax. Therefore, in subsequent experiments, we adjusted the personalization parameters (duplications, participation frequencies, and weights) so that the resulting sensitivities relate to the actual budgets.

*E.g.* let  $\varepsilon_1, \varepsilon_2 \in \mathbb{R}_+$  be two DP budgets with  $\varepsilon_2 = c \cdot \varepsilon_1$  for any  $c > 1$ . Then, for the uGNMax, the duplications  $u_2$  of points having the higher budget  $\varepsilon_2$  are set to  $u_2 := c \cdot u_1$  where  $u_1$  is the number of duplications for points having the lower budget. For vGNMax, the participation frequency  $s_1$  of teachers trained on points having the lower budget  $\varepsilon_1$  is set to  $s_1 := 1/c^2$  while the frequency  $s_2$  of teachers trained on points having the higher budget is always one<sup>3</sup>. Finally, for the wGNMax, the weights of teachers are set to the corresponding budgets and then normalized so that the sum of all weights equals the number of teachers. Thus,  $w_1 := \varepsilon_1/\bar{w}$  and  $w_2 := \varepsilon_2/\bar{w}$  where  $\bar{w}$  is the average weight of all teachers.

A comprehensive rationale on parameter settings for our personalized variants as well as a description of further implementation details is left to Appendix B.

### 5.2 Advantage of Personalization

To better understand how much privacy the generation of labels consumes on both data groups (lower and higher privacy), we tracked the privacy costs over the course of generating 2,000 labels on both datasets for our three novel PATE variants. Figure 2 and Figure 3 (Appendix C) depict the results over various personalized privacy distributions for the MNIST and Adult income dataset, respectively. For comparison, the costs of non-personalized GNMax over the produced labels are inserted into the plots.

We observe two separate lines of privacy cost history per variant. As a general trend, as expected, both lines differ more the more the individual budgets differ. This effect also increases when the proportion of sensitive data with the higher budget decreases. Moreover, with increasing ratio of the higher budget, both costs grow slower. Another observation is that the cost histories of the uGNMax and the wGNMax almost behave equally for all budget distributions. In contrast, vGNMax produces significantly less labels than the other two variants in every experiment and often times even yields less labels than non-personalized PATE.

To evaluate the number of labels that can actually be generated for the given privacy budget distribution, we have to count how many labels are returned before any data point’s privacy budget is exceeded. In Figure 2 and Figure 3 (Appendix C), this corresponds to the moment when either the lower costs reach the lower budget or the higher costs reach the higher budget, whatever happens first. The resulting numbers of produced labels over the experiments are shown in Table 3 for the MNIST dataset against the minimum baseline. A version of this table including all three baselines (minimum, maximum, average) and one table depicting the results for Adult income data can be found in Appendix C (see Table 4 and Table 5). In comparison to the minimum baseline, upsampling and weighting produce more labels.

When considering the number of produced labels in the voting process, the utility advantage of our personalized PATE over the non-personalized variant becomes visible. For half of the sensitive MNIST data having a budget of  $\log 4$  and the other half having  $\log 2$ , 239 labels can be produced by personalized PATE, instead of 99 in the case of non-personalized PATE. This leads to a student accuracy of 90.78% while non-personalized PATE only achieves 84.51%. Analogously, on Adult income data, 203 labels can be produced, leading to a student accuracy of 81.76%. Non-personalized PATE, instead, produces 88 labels so that the student only achieves an accuracy of 79.85%.

Our results are not directly comparable to those of [16] since in contrast to their work, we did not apply virtual adversarial training but only used the public data. Their final models’ accuracy is 98.5% on MNIST with  $\varepsilon = 1.97$  while our student model never surpassed 95% even for a privacy budget of  $\varepsilon = \log 16 \approx 2.77$ . We decided not to

<sup>3</sup>We set  $s_1 := 1/c^4$  for vGNMax in our experiments so that different privacy budgets exhausted approximately at the same time.

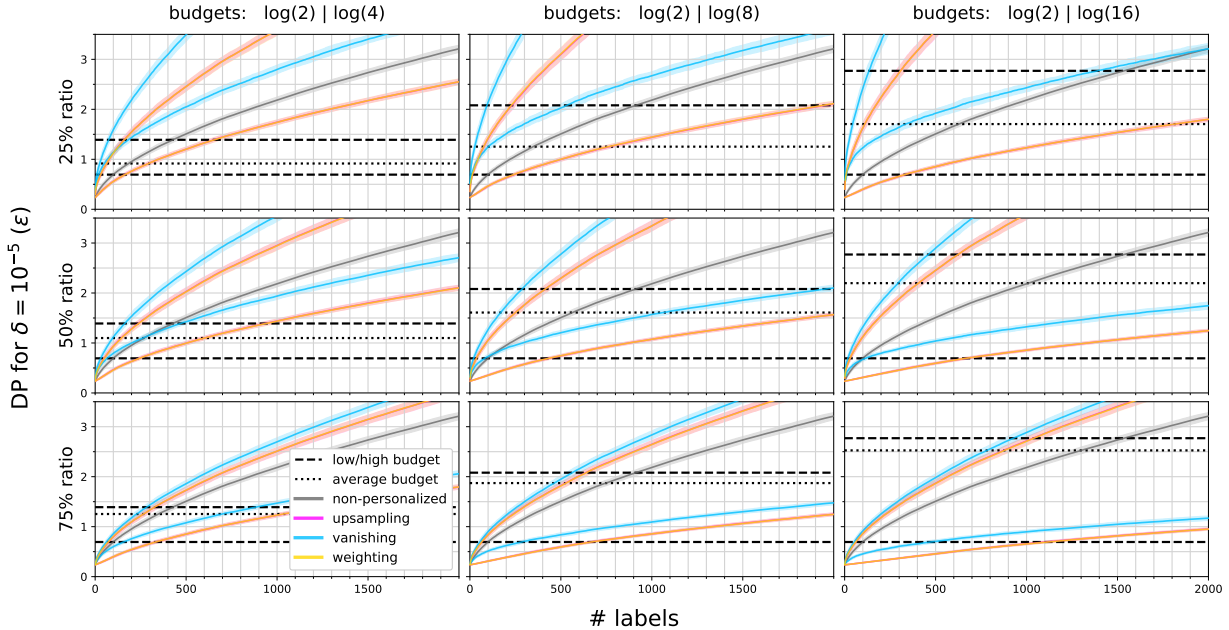


Figure 2: **Privacy Cost History (MNIST)**. Costs for generating the first 2,000 labels. Results are averaged over five voting processes by ten teacher ensembles, each for different budget distributions and GNMax variants upsampling, vanishing, and weighting. Privacy costs and budgets are given in  $(\epsilon, \delta)$ -DP for  $\delta = 10^{-5}$ . Ratios indicate the proportion of data with the higher budget. Costs are listed per group of data points sharing the same budget.

integrate the adversarial training method in order to study the pure effect of our personalization method and exclude any other effects on the resulting model utility. However, our method still outperforms [16] when it comes to label generation: In [16], 286 labels were produced on the MNIST dataset, while our non-personalized PATE produced more than 650 labels for the same privacy budget. Additionally, our generated labels are even more accurate when evaluating them against ground truth ( $\approx 97.7\%$ ) than theirs (93.18%).

Note that the budget combinations log 4 with 75% and log 8 with 25% yield the same average privacy budget. Nevertheless, the experiment on distribution log 4 with 75% yields slightly more labels and higher accuracy than that on log 8 with 25%. This might indicate that having a smaller gap between the lower and the higher privacy budget yields increased performance, and that it might be better to have more data points with slightly higher privacy budgets than a few data points with very high privacy budgets.

higher budget in $\epsilon$	25% ratio			50% ratio			75% ratio		
	u	v	w	u	v	w	u	v	w
log 4	158	25	158	237	67	239	326	157	326
log 8	231	0	229	414	84	414	636	285	638
log 16	308	0	308	623	115	623	1,038	477	1,041
baseline	99								

Table 3: **Labels per Personalization (MNIST)**. Number of produced labels. Results depict the average over five voting processes by ten teacher ensembles each for different budget distributions and GNMax variants (**upsampling**, **vanishing**, **weighting**). Non-personalized GNMax using the minimum budget serves as baseline. The voting accuracies of all experiments are  $\approx 97.7\%$ . Inherent inefficiencies of vanishing PATE led to exhaustion before any label was produced in two cases.

### 5.3 Compensating Underrepresented Data

We aimed to evaluate the influence of giving a higher privacy budget only to (parts of) the underrepresented class in the Adult income dataset. The numbers of produced labels as well as voting accuracies, and the precision and recall values of teachers that were achieved in our experiments are depicted in Table 6 and Table 7 in Appendix C, respectively. Regarding the numbers of produced labels, we observe similar relations and trends as for the experiments described in Section 5.2. This stands in stark contrast to the student accuracies which decrease for greater amounts of

budgets. However, when setting the higher privacy budget to  $\log 4$ , we observe slightly better student accuracies than the baselines which indicates that a minor increase in the information usage of the underrepresented class leads to an optimal balance between the representations of both classes.

For all budget distributions, the precision (ratio of true predictions among all positive predictions) of teachers is smaller than that for non-personalized experiments and decreases with increasing budgets. Conversely, the recall (ratio of true predictions among all positives) is higher than that for non-personalized experiments and increases with increasing budgets. These two observations point that the higher the amounts of budgets for data of the minority class, the more frequently that class gets predicted.

## 6 Related Work

This section presents related work about personalized DP and privacy-preserving ML techniques.

### 6.1 Techniques for Personalized DP

Several techniques to allow for personalized privacy accounting in DP outside of the scope of ML have been proposed, so far. The methods were designed for application in privacy-preserving data aggregation methods in the database context and are, therefore, not directly applicable to ML.

One of the first techniques for personalized DP was proposed by Alaggar *et al.* [31]. Their *stretching mechanism* scales data points individually before they are perturbed by noise. Thus, the noise affects each point with individual intensity. Jorgensen *et al.* invented two other methods [30]. Their *sample mechanism* excludes particular data points from being processed with probability according to their privacy preferences. In contrast, their *personalized exponential mechanism* determines the probabilities of processing results according to personalized privacy requirements. These probabilities are then used to randomly select the processing result for a dataset. Two *partitioning algorithms* were proposed by Li *et al.* [38] that separately process groups of sensitive data each with an individual privacy expenditure. Note that our vanishing and weighting mechanisms were inspired by the sample mechanism and the stretching mechanism, respectively.

### 6.2 DP Mechanisms for ML

PATE is not the only approach that can be used to apply DP in ML workflows. Another commonly used approach is the *Differentially Private Stochastic Gradient Descent (DP-SGD)* [11]. In DP-SGD, privacy is achieved by first limiting the changes to an ML model that each individual data point can cause. This is done by clipping model gradients on a per-example basis during training. Then, to achieve DP guarantees, noise is added to the gradients before the model parameters are updated with them. Privacy costs of DP-SGD are accounted through the *moments accountant* [19]. In this approach, multiple moments of the privacy loss random variable are calculated to obtain a DP bound by using the standard Markov inequality.

The initial non-personalized DP-SGD algorithm was extended by Feldman and Zrnic to account individual privacy costs per data point using an *RDP filter* [13]. An RDP filter applies RDP bounds and removes data points from training when their individual privacy budget is exhausted. Jordon *et al.* personalized the moments accountant by dividing it into an *upwards* and a *downwards moments accountant* which are composed to a *personalized moments accountant* to provide data-dependent DP bounds individually per data point [39]. In contrast to our personalized variants, their mechanism only performs individual accounting of privacy costs but does not implement measures to specify per-data point privacy budgets before training.

## 7 Discussion and Future Work

This section discusses the results generated in this work and provides an outlook on possible future research directions.

### 7.1 Improving Utility with Personalized PATE

Particularly in sensitive domains such as in health care, using high utility ML models is crucial since low utility models and their incorrect decisions might have severe consequences. Therefore, many parties still resign from using DP in their sensitive ML applications or set a very high privacy budget for all data points, which results in low privacy protection for the underlying data.

The introduction of personalized PATE involves multiple benefits. First of all, our methods allow to integrate PATE in a system where individuals whose data get collected can choose what privacy level they want this data to be treated with. That option alone might make individuals more willing to share their data. This would lead to an increased availability of training data for the PATE teacher models. According to recent research, such an increased availability of data has positive effects on the model utility when training with DP [40]. Additionally, our experiments have shown that supporting different privacy budgets within PATE can yield higher utility models since it prevents from having to always comply with the most strict privacy requirements encountered in a dataset. For the MNIST dataset, we observe that when as little as 25% of the data points specify a privacy budget of  $\log 4$  instead of  $\log 2$ , more than 150% the original amount of labels can be generated (*cf.* Table 3). When further increasing the privacy budget for that small data population or including more data points with that budget into the training, in our experiments, up to ten times the amount of labels could be generated. In general, depending on the privacy budget distributions, even obtaining more labels becomes possible. This is due to the fact that the data points with higher privacy budgets can contribute more information while privacy of data points with higher protection requirements can be spared.

## 7.2 Comparison of Personalized PATE Variants

In the practical comparison of our three PATE variants, we see that the upsampling and weighting variants constantly outperform the vanishing approach. This can be explained by the fact that the vanishing approach leads to the absence of teachers in a voting. As a consequence, the voting accuracy drops due to the greater relative impact of noise on the fewer teacher votes. To avoid this effect and align the voting accuracy with that of other experiments, we decreased the noise intensity which led to higher privacy expenditure. It seems that the vanishing approach of sparing the privacy of data is inefficient.

The weighting and upsampling approach do not yield significant differences in performance during our experiments. Upsampling might, however, offer greater flexibility in the individual choice of privacy budgets. This is because weighting is performed on a per-teacher basis. Hence, the privacy costs of all data points used to train the same teacher are the same, whereas upsampling enables setting unique per-point budgets. Of course, weighting can still be used even if potentially every data point has a different privacy budget. In that case, points with similar privacy budgets could be grouped into one teacher, and the privacy budget of that teacher should be set to comply with the strictest requirement among all its training data points. However, this would result in a waste of privacy budgets among all data points with higher privacy budgets within this teacher that would potentially allow for more privacy consumption.

The upsampling approach comes at the price of higher resource consumption due to larger amounts of training data. This data can be used to (1) potentially increase the amount of training data per teacher, or (2) increase the number of teachers. (1) results in increased teacher accuracies, whereas (2) allows to use higher amounts of noise in the voting process, *i.e.* lower privacy costs, without loss of voting accuracy. Both effects stand in direct relation since the more teachers are used, the less training data per teacher is available. To preserve the optimal point-to-teacher ratio, more teachers have to be trained on duplicated data. Additionally, since duplication of data has to be aligned to relations between this data’s different privacy budgets, even points with the lowest budgets might have to be duplicated. Detailed insights are explained in Appendix B.

Note that one great advantage of our personalized PATE variants is that they could also be combined during a voting process. For example towards the end of a label generation process if not all privacy budgets are exceeded at the exact same time, the vanishing variant could be applied to exploit remaining budgets while sparing the exhausted.

## 7.3 Underrepresented Classes and Outliers

In this work, we have also looked into the question if performance can be enhanced when only very small but expressive parts of the data contribute more private information. As shown in Table 6 (Appendix C), the improvements are only marginally. Beyond that, looking at the recall and precision of the resulting models provides the insight that data with higher privacy budgets has a direct influence on what classes the student model predicts. We find that to be an interesting observation since it suggests that through privacy budget assignment, it might be possible to either mitigate or to enforce biases in the data. Hence, the assignment of individual privacy budgets plays a vital role and its effect should be evaluated very carefully.

Another question that arises is the one of why should individual data holders volunteer to contribute their data with lower privacy guarantees than other data holders. In particular data holders who hold outlier data might usually demand higher privacy guarantees. Therefore, with our personalized PATE variants, it might become even harder for the student model to learn any information about this data. We argue that this is why personalized PATE should be included in a system that collects data holders’ consent based on their understanding of the effect of different privacy levels, both on their personal risk of privacy leakage and improved utility of the models. When the data holders see

that increasing their personal privacy risk very little might yield in an overall improvement of the service that they also benefit from, such as improved health care, they might agree to contributing more of their information. Additionally, the personalized PATE variants allow us to combine data from different datasets and data sources. In particular, they can be used to train a model on a combination of existing publicly available datasets without any privacy restrictions and additional datasets that hold data with (varying) privacy requirements, based on the purpose and consent during the collection of the respective datasets. Without personalized DP variants, a joint PATE training on them would have required setting the privacy budget to the lowest value encountered among all data sources. Due to our personalization, we can employ different privacy budgets, and, thereby, yield higher utility.

#### **7.4 Outlook and Future Directions**

Based on the insights on the potential of personalized privacy budgets being able to create or enforce biases in a dataset, future work should focus on combining the privacy and utility aspects of this work with considerations on biases fairness. This could be done by balancing information of different parts of the data distribution of interest to satisfy fairness aspects and ultimately to optimize utility. Such a balance could, for example, be achieved by not always exploiting the complete privacy budgets available for some data points.

In addition, further theoretical research on improving the tight bound for privacy analysis of PATE would be helpful to obtain more realistic estimates of the privacy costs during the voting process. The current analysis assumes that each data point could fully change its teacher model's prediction. In most scenarios, this assumption is, however, too strong. With a tighter estimate of a data point's influence, each vote would consume less privacy budget, and as a consequence more labels could be produced.

Moreover, it would be of interest to study how applications of distributed PATE and similar frameworks, *e.g.* [41], where the training data is distributed over different entities, could benefit from our personalized aggregation mechanisms. Our mechanisms could be applied there to implement both individual data point privacy requirements, but also different organisational requirements between the different entities, and thereby, allow for more meaningful cooperative training and models of higher utility.

Finally, it will be interesting to study the behavior of our novel personalized PATE variants further, also with more complex privacy budget distributions within the dataset. We see the biggest challenge for this part in the fine-tuning of the parameters and the combination of the mechanisms such that all privacy budgets among the data points can be completely exhausted for maximal utility.

### **8 Conclusion**

Preserving privacy for the training data in ML is a crucial topic. Often, this privacy is achieved at the costs of the final model's utility. To improve the privacy-utility trade-off, we proposed three novel variants for the PATE algorithm that allow for the use of personalized privacy budgets among the data points. We formally defined our three variants, conducted theoretical analyses of their privacy bounds, and experimentally evaluated their effect on PATE's utility for two different datasets and different privacy budget distributions within them. Our results show that through personalization in PATE, we were able to generate up to ten times more labels in comparison to the standard approach that would have to comply to the highest privacy requirements encountered in a dataset. The increased amount of labels also translates into significant improvements in the student model's accuracy. Our personalized PATE variants are, therefore, able to mitigate the loss of utility that is usually introduced by DP.

### **9 Acknowledgements**

This work is supported by the German Federal Ministry of Education and Research (grant 16SV8463: WerteRadar).

## References

- [1] Jenna Wiens and Erica S Shenoy. Machine learning for healthcare: on the verge of a major shift in healthcare epidemiology. *Clinical Infectious Diseases*, 66(1):149–153, 2018.
- [2] Min Chen, Yixue Hao, Kai Hwang, Lu Wang, and Lin Wang. Disease prediction by machine learning over big data from healthcare communities. *Ieee Access*, 5:8869–8879, 2017.
- [3] Maxwell W Libbrecht and William Stafford Noble. Machine learning applications in genetics and genomics. *Nature Reviews Genetics*, 16(6):321–332, 2015.
- [4] Ali A Mahmoud, Tahani AL Shawabkeh, Walid A Salameh, and Ibrahim Al Amro. Performance predicting in hiring process and performance appraisals using machine learning. In *2019 10th International Conference on Information and Communication Systems (ICICS)*, pages 110–115. IEEE, 2019.
- [5] Reza Shokri, Marco Stronati, Congzheng Song, and Vitaly Shmatikov. Membership inference attacks against machine learning models. In *2017 IEEE Symposium on Security and Privacy (SP)*, pages 3–18. IEEE, 2017.
- [6] Matt Fredrikson, Somesh Jha, and Thomas Ristenpart. Model inversion attacks that exploit confidence information and basic countermeasures. In *Proceedings of the 22nd ACM SIGSAC conference on computer and communications security*, pages 1322–1333, 2015.
- [7] Karan Ganju, Qi Wang, Wei Yang, Carl A Gunter, and Nikita Borisov. Property inference attacks on fully connected neural networks using permutation invariant representations. In *Proceedings of the 2018 ACM SIGSAC conference on computer and communications security*, pages 619–633, 2018.
- [8] Cynthia Dwork. Differential privacy. In *International Colloquium on Automata, Languages, and Programming*, pages 1–12. Springer, 2006.
- [9] Eugene Bagdasaryan, Omid Poursaeed, and Vitaly Shmatikov. Differential privacy has disparate impact on model accuracy. *Advances in Neural Information Processing Systems*, 32:15479–15488, 2019.
- [10] Nicolas Papernot, Abhradeep Thakurta, Shuang Song, Steve Chien, and Úlfar Erlingsson. Tempered sigmoid activations for deep learning with differential privacy. *Proceedings of the AAAI Conference on Artificial Intelligence*, 35(10):9312–9321, May 2021. URL <https://ojs.aaai.org/index.php/AAAI/article/view/17123>.
- [11] Shuang Song, Kamalika Chaudhuri, and Anand D. Sarwate. Stochastic gradient descent with differentially private updates. In *2013 IEEE Global Conference on Signal and Information Processing*, pages 245–248, 2013. doi:10.1109/GlobalSIP.2013.6736861.
- [12] Nicolas Papernot, Martín Abadi, Úlfar Erlingsson, Ian Goodfellow, and Kunal Talwar. Semi-supervised knowledge transfer for deep learning from private training data. In *Proceedings of the International Conference on Learning Representations*, 2017. URL <https://arxiv.org/abs/1610.05755>.
- [13] Vitaly Feldman and Tijana Zrnic. Individual privacy accounting via a renyi filter. In *Thirty-Fifth Conference on Neural Information Processing Systems*, 2021.
- [14] Yann LeCun and Corinna Cortes. MNIST handwritten digit database. <http://yann.lecun.com/exdb/mnist/>, 2010. URL <http://yann.lecun.com/exdb/mnist/>.
- [15] Ronny Kohavi and Barry Becker. Adult data set. *UCI machine learning repository*, 5:2093, 1996.
- [16] Nicolas Papernot, Shuang Song, Ilya Mironov, Ananth Raghunathan, Kunal Talwar, and Úlfar Erlingsson. Scalable private learning with pate. In *International Conference on Learning Representations (ICLR)*, 2018. URL <https://arxiv.org/abs/1802.08908>.
- [17] Takeru Miyato, Shin-Ichi Maeda, Masanori Koyama, and Shin Ishii. Virtual adversarial training: A regularization method for supervised and semi-supervised learning. *IEEE Transactions on Pattern Analysis and Machine Intelligence*, 41(8):1979–1993, 2019. doi:10.1109/TPAMI.2018.2858821.
- [18] David Berthelot, Nicholas Carlini, Ian Goodfellow, Nicolas Papernot, Avital Oliver, and Colin Raffel. Mixmatch: A holistic approach to semi-supervised learning, 2019.
- [19] Martin Abadi, Andy Chu, Ian Goodfellow, H Brendan McMahan, Ilya Mironov, Kunal Talwar, and Li Zhang. Deep learning with differential privacy. In *Proceedings of the 2016 ACM SIGSAC Conference on Computer and Communications Security*, pages 308–318, 2016.
- [20] Peter Sörries, Claudia Müller-Birn, Katrin Glinka, Franziska Boenisch, Marian Margraf, Sabine Sayegh-Jodehl, and Matthias Rose. Privacy needs reflection: Conceptual design rationales for privacy-preserving explanation user interfaces. *Mensch und Computer 2021-Workshopband*, 2021.
- [21] Maximilian Teltzrow and Alfred Kobsa. Impacts of user privacy preferences on personalized systems. In *Designing personalized user experiences in eCommerce*, pages 315–332. Springer, 2004.



- [22] Jan Kolter and Günther Pernul. Generating user-understandable privacy preferences. In *2009 International Conference on Availability, Reliability and Security*, pages 299–306. IEEE, 2009.
- [23] Sandra Wachter, Brent Mittelstadt, and Chris Russell. Counterfactual explanations without opening the black box: Automated decisions and the gdpr. *Harv. JL & Tech.*, 31:841, 2017.
- [24] Aiping Xiong, Tianhao Wang, Ninghui Li, and Somesh Jha. Towards effective differential privacy communication for users’ data sharing decision and comprehension. In *2020 IEEE Symposium on Security and Privacy (SP)*, pages 392–410. IEEE, 2020.
- [25] Chris Jay Hoofnagle and Jennifer M Urban. Alan westin’s privacy homo economicus. *Wake Forest L. Rev.*, 49: 261, 2014.
- [26] Karthik S Bhat and Neha Kumar. Sociocultural dimensions of tracking health and taking care. *Proceedings of the ACM on Human-Computer Interaction*, 4(CSCW2):1–24, 2020.
- [27] Cynthia Dwork. Differential privacy: A survey of results. In *International conference on theory and applications of models of computation*, pages 1–19. Springer, 2008.
- [28] Cynthia Dwork, Aaron Roth, et al. The algorithmic foundations of differential privacy. *Foundations and Trends in Theoretical Computer Science*, 9(3-4):211–407, 2014.
- [29] Ilya Mironov. Rényi differential privacy. In *2017 IEEE 30th Computer Security Foundations Symposium (CSF)*, pages 263–275. IEEE, 2017.
- [30] Zach Jorgensen, Ting Yu, and Graham Cormode. Conservative or liberal? personalized differential privacy. In *2015 IEEE 31st international conference on data engineering*, pages 1023–1034. IEEE, 2015.
- [31] Mohammad Alaggan, Sébastien Gambs, and Anne-Marie Kermarrec. Heterogeneous differential privacy. *arXiv preprint arXiv:1504.06998*, 2015.
- [32] Hamid Ebadi, David Sands, and Gerardo Schneider. Differential privacy: Now it’s getting personal. *Acm Sigplan Notices*, 50(1):69–81, 2015.
- [33] Yu-Xiang Wang. Per-instance differential privacy. *Journal of Privacy and Confidentiality*, 9(1), 2019.
- [34] Nicolas Papernot. Implementation of an rdp privacy accountant and smooth sensitivity analysis for the pate framework, 2018. URL [https://github.com/tensorflow/privacy/tree/master/research/pate\\_2018](https://github.com/tensorflow/privacy/tree/master/research/pate_2018).
- [35] Guido Van Rossum and Fred L. Drake. *Python 3 Reference Manual*. CreateSpace, Scotts Valley, CA, 2009. ISBN 1441412697.
- [36] Jason Brownlee. How to develop a cnn for mnist handwritten digit classification, 2019. URL <https://machinelearningmastery.com/...>
- [37] Vinith M Suriyakumar, Nicolas Papernot, Anna Goldenberg, and Marzyeh Ghassemi. Chasing your long tails: Differentially private prediction in health care settings. In *Proceedings of the 2021 ACM Conference on Fairness, Accountability, and Transparency*, pages 723–734, 2021.
- [38] Haoran Li, Li Xiong, Zhanglong Ji, and Xiaoqian Jiang. Partitioning-based mechanisms under personalized differential privacy. In *Pacific-Asia Conference on Knowledge Discovery and Data Mining*, pages 615–627. Springer, 2017.
- [39] James Jordon, Jinsung Yoon, and Mihaela van der Schaar. Differentially private bagging: Improved utility and cheaper privacy than subsample-and-aggregate. In *Advances in Neural Information Processing Systems*, pages pp. 4323–4332, 2019.
- [40] Florian Tramèr and Dan Boneh. Differentially private learning needs better features (or much more data). *arXiv preprint arXiv:2011.11660*, 2020.
- [41] Christopher A Choquette-Choo, Natalie Dullerud, Adam Dziedzic, Yunxiang Zhang, Somesh Jha, Nicolas Papernot, and Xiao Wang. Capc learning: Confidential and private collaborative learning. *arXiv preprint arXiv:2102.05188*, 2021.

## A Additional Background on RDP and PATE

This section supplements Section 2 by providing formalizations of Rényi divergence, RDP composition, and the tight bound.

### Rényi Differential Privacy

**Definition 10** (cf. [29], Def. 3). Let  $P$  and  $Q$  be two probability distributions over  $\mathcal{D}$ . Rényi divergence of order  $\alpha \in \mathbb{R}_+ \setminus \{1\}$  for  $P$  and  $Q$  can be defined as

$$\mathbb{D}_\alpha [P \parallel Q] := \frac{1}{\alpha - 1} \cdot \log \mathbb{E}_{x \sim Q} \left[ \left( \frac{P(x)}{Q(x)} \right)^\alpha \right], \quad (14)$$

where  $x \sim Q$  expresses that samples  $x \in \mathcal{D}$  follow the probability distribution  $Q$ .

Composition under RDP can be expressed with the following composition theorem.

**Lemma 3** (cf. [29], Prop. 1). Let  $\mathcal{R}_1, \mathcal{R}_2$  be arbitrary result spaces. Let further  $M_1: \mathcal{D}^* \rightarrow \mathcal{R}_1, M_2: \mathcal{D}^* \rightarrow \mathcal{R}_2$  be mechanisms that satisfy  $(\alpha, \varepsilon_1)$ - and  $(\alpha, \varepsilon_2)$ -RDP, respectively. Then, the composition  $M_3(D) \mapsto (M_1(D), M_2(D))$  satisfies  $(\alpha, \varepsilon_1 + \varepsilon_2)$ -RDP.

Note that Lemma 3 also holds for adaptive sequential composition as shown in [29]. RDP guarantees can be transformed into DP guarantees as follows.

**Lemma 4** (cf. [29], Prop. 3). Let  $M: \mathcal{D}^* \rightarrow \mathcal{R}$  be an  $(\alpha, \varepsilon)$ -RDP mechanism. Then,  $M$  also satisfies  $(\varepsilon', \delta)$ -DP with

$$\varepsilon' = \varepsilon + \frac{\ln 1/\delta}{\alpha - 1} \quad (15)$$

for all  $\delta \in (0, 1]$ .

Lemma 3 and Lemma 4 are proven in [29].

### Tight Bound Privacy Analysis of PATE

The tight bound for PATE can be defined as follows.

**Lemma 5** (cf. [16], Thm. 6). Let  $M$  simultaneously satisfy  $(\alpha_1, \varepsilon_1)$ -RDP and  $(\alpha_2, \varepsilon_2)$ -RDP. Both RDP bounds can be computed by applying the loose bound for two different alpha values. Suppose that  $1 \geq q \geq \mathbb{P}[M(D) \neq j^*]$  holds for a likely teacher voting  $j^*$ . Additionally suppose that  $\alpha \leq \alpha_1$  and  $q \leq \exp((\alpha_2 - 1) \cdot \varepsilon_2) / \left( \frac{\alpha_1}{\alpha_1 - 1} \cdot \frac{\alpha_2}{\alpha_2 - 1} \right)^{\alpha_2}$ . Then,  $M$  satisfies  $(\alpha, \varepsilon)$ -RDP for any neighboring dataset  $D'$  of  $D$  with

$$\varepsilon = \frac{1}{\alpha - 1} \cdot \log ((1 - q) \cdot A + q \cdot B), \quad (16)$$

where  $A$  and  $B$  are defined as follows.

$$A := \left( \frac{1 - q}{1 - (q \cdot e^{\varepsilon_2})^{\frac{\alpha_2 - 1}{\alpha_2}}} \right)^{\alpha - 1}, \quad (17)$$

$$B := \left( \frac{e^{\varepsilon_1}}{q^{\frac{1}{\alpha_1 - 1}}} \right)^{\alpha - 1}. \quad (18)$$

This holds since according to [16], Prop. 7, for a GNMax aggregator  $M$  with parameter  $\sigma$  and for any class  $j^* \in \mathcal{Y}$  the following statement applies.

$$\mathbb{P}[M(D) \neq j^*] \leq \frac{1}{2} \sum_{j \neq j^*} \operatorname{erfc} \left( \frac{n_{j^*} - n_j}{2\sigma} \right) \quad (19)$$

where  $\operatorname{erfc}(\cdot)$  denotes the complementary error function defined by

$$\operatorname{erfc}(a) := \frac{2}{\sqrt{\pi}} \int_a^\infty e^{-t^2} dt. \quad (20)$$

See [16] for the proofs.

## B Implementation Details of the Personalized Variants

This section contains details on the implementation of the personalized GNMax variants which were left out in Sections 3 and 4 for the sake of brevity.

The general goal of the practical implementation of our variants is to make sure that their general parameters align. Thus, the optimization of PATE hyperparameters, *i.e.* number of teachers  $k$ , noise standard deviation for consensus checks  $\sigma_1$ , noise standard deviation for label creation  $\sigma_2$ , and threshold for consensus checks  $T$ , is maintained and different variants become comparable.

### Details of Upsampling

Upsampling PATE extends the training data for teachers by duplicates. Figure 4 shows that the ratio of privacy costs approaches the ratio of their corresponding budgets after some votings. Therefore, numbers of duplicates should align to the relation of privacy budgets. This can be achieved by initializing the numbers of duplicates as the different budgets and then scaling them up equally until each of them reaches an integer with some desired precision. Note that a higher precision might lead to very high numbers of duplicates if not all budgets are multiples of each other as in our experiments.

Let  $N$  and  $N'$  be the numbers of sensitive data and sensitive data enlarged by duplicates, respectively. Then we can define the relative gain of training data as  $s := N'/N$ . To ensure the same accuracy of teachers as in non-personalized PATE, the number of teachers  $k$  has to be scaled by  $s$ . The remaining PATE hyperparameters  $\sigma_1, \sigma_2, T$  have to be scaled by  $s$  as well to achieve a comparable voting accuracy and privacy efficiency as for non-personalized PATE.

### Details of Vanishing

Vanishing PATE differentiates privacy on teacher-level by avoiding participation in some votings. Therefore, sensitive data has to be grouped budget-wise and then be given to teachers *s.t.* all data points in a teacher have (almost) the same privacy budget. Afterwards, the participation frequencies have to be set according to the lowest budget of each teacher. Figure 4 suggests that the frequencies corresponding to two different budgets should have a relation that is at least quadratic to the relation of their corresponding budgets. In our experiments we used a relation that equals the relation of budgets to the power of four since the costs of data with different budgets are closer after a few votings before they approach constant ratios as for upsampling and weighting. So we initialized frequencies to the corresponding budgets, squared them, and finally divided them by the highest frequency so that frequencies were probabilities and the highest one was 100%.

In order to be comparable to the other personalized variants, the voting accuracy of vanishing PATE should be retained by decreasing the noise intensity according to the smaller number of voting teachers. A weaker noise entails higher privacy costs for participating teachers' data. Experiments showed that the privacy costs of all data is lower if the number of participating is stable over the whole voting process. Therefore, our implementation maintains a stable number of participating teachers by selecting random alternations that are changed periodically. More precisely, randomly selected sets of teachers participate periodically in votings where the period aligns to their frequency and equal periods are shifted to achieve a stable number of participating teachers per voting. After some votings, new sets of teachers with identical frequencies are randomly sampled to reduce the risk of biases that could be introduced into labels by cliques of teachers with similar knowledge.

### Details of Weighting

The weighting approach does not change PATE hyperparameters in contrast to the other personalized variants. Nonetheless, sensitive data has to be grouped budget-wise before being provided to the teachers as in vanishing PATE. The teachers are then given weights according to the budgets *s.t.* all weights sum up to the number of teachers. Following Figure 4, weights can be set to their corresponding budgets divided by the average budget. Thus, all hyperparameters can remain unchanged while their optimization regarding the accuracy of teachers and voting still holds.

### Efficient Handling of Personalized Privacy

The consideration of different privacy budgets and costs increases the complexity of PATE both in time and space. To counteract this problem, privacy costs can be calculated and stored group-wise. That is all data which has the same number of duplicates in the case of upsampling. In the vanishing approach, the data of all participating teachers have the same costs in a voting. However, costs have to be stored and accumulated teacher-wise. Usually, weighting PATE

has the lowest complexity since all costs can be calculated, accumulated, and stored per group of data having the same budget.

## C Additional Results

Results of experiments on the Adult income dataset as well as more comprehensive results of MNIST experiments are presented here.

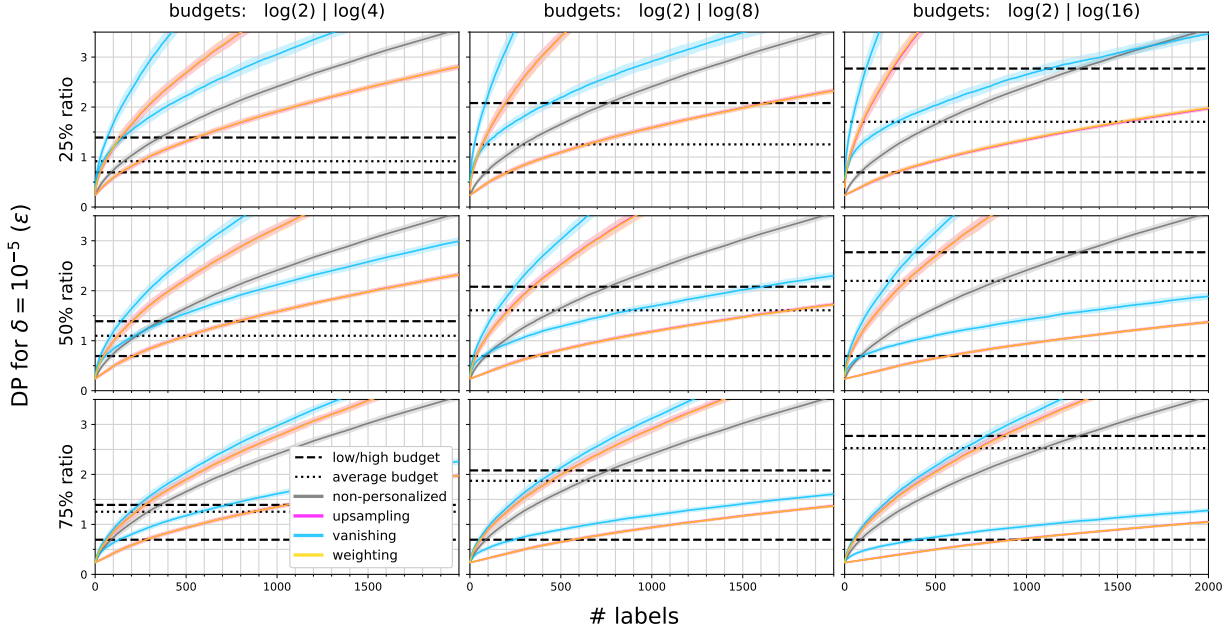


Figure 3: **Privacy Cost History (Adult)**. Costs for generating the first 2,000 labels. Results are averaged over five voting processes by ten teacher ensembles, each for different budget distributions and GNMax variants upsampling, vanishing, and weighting. Privacy costs and budgets are given in  $(\epsilon, \delta)$ -DP for  $\delta = 10^{-5}$ . Ratios indicate proportion of data with the data have the higher budget. Costs are given per group of points that share the same budget.

higher budget in $\epsilon$	# produced labels										
		25% ratio			50% ratio			75% ratio			
baselines	min	u	v	w	u	v	w	u	v	w	max
log 4	99	158	25	158	237	67	239	326	157	326	426
		average			average			average			
log 8	99	231	0	229	414	84	414	636	285	638	914
		average			average			average			
log 16	99	308	0	308	623	115	623	1,038	477	1,041	1,540
		average			average			average			

Table 4: **Labels per Personalization with Multiple Baselines (MNIST)**. Number of produced labels. Results depict the average over five voting processes by ten teacher ensembles each for different budget distributions and GNMax variants (**upsampling**, **vanishing**, **weighting**). Non-personalized experiments (with minimum, average, or maximum budget) serve as baselines. Due to inherent inefficiencies of vanishing PATE, no label could be produced before exhaustion in two cases.

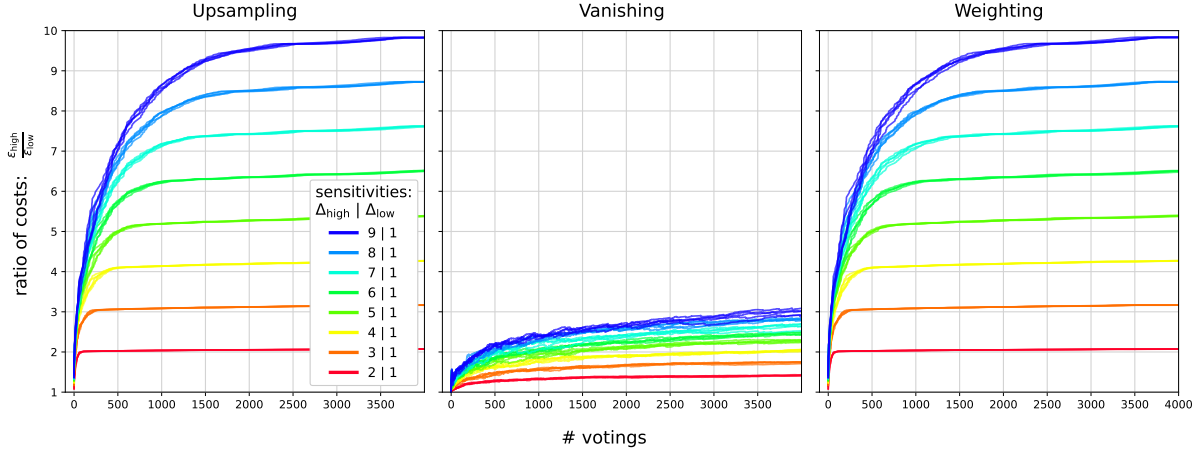


Figure 4: **Adjustment of Parameters for Personalized Variants.** Privacy cost relation between two equal-sized groups of sensitive data (high and low sensitivity) shown over 4,000 votings on the MNIST dataset for each of our three personalized Confident-GNMax variants. All costs are given in  $(\epsilon, \delta)$ -DP for  $\delta = 10^{-5}$ . Each of ten teacher ensembles was used to vote five times for all labels in the public dataset that was shuffled differently for each combination. After some votings, the ratio of different costs almost remains constant at the ratio of corresponding sensitivities. Note that the sensitivities shown are only proportions of sensitivities. This means that for upsampling and weighting, the *plain* sensitivities were scaled while for vanishing, *average* sensitivities, *i.e.* participation frequencies, were scaled and depicted.

higher budget in $\epsilon$ baselines	# produced labels										
	min	25% ratio			50% ratio			75% ratio			max
		u	v	w	u	v	w	u	v	w	
log 4	88	140	16	139	202	57	203	272	133	273	354
log 8	88	198	10	198	346	75	349	541	236	543	763
log 16	88	264	8	259	530	95	530	868	400	872	1,288

Table 5: **Labels per Personalization with Multiple Baselines (Adult).** Number of produced labels. Results depict the average over five voting processes by ten teacher ensembles each for different budget distributions and GNMax variants (**upsampling**, **vanishing**, **weighting**). Non-personalized experiments (with minimum, average, or maximum budget) serve as baselines.

higher budget in $\epsilon$ baselines	# produced labels					
	min	25% ratio	50% ratio	75% ratio	100% ratio	max
		average	average	average	average	
log 4	88	90	95	101	109	354
log 8	88	93	108	132	162	763
log 16	88	96	129	172	225	1,288

Table 6: **Labels per Skew Personalization (Adult).** Number of produced labels. Results depict the average over five voting processes by ten teacher ensembles using **upsampling** each for different budget distributions (higher budget & its ratio among minority data). Non-personalized experiments with minimum, average, or maximum budget serve as baselines.

higher budget in $\epsilon$	25% ratio			50% ratio			75% ratio			100% ratio		
	accuracy	precision	recall	accuracy	precision	recall	accuracy	precision	recall	accuracy	precision	recall
log 4	86.68	65.92	56.05	86.61	63.12	61.70	86.19	60.85	66.24	85.64	58.95	69.68
log 8	86.60	63.14	61.73	85.64	58.94	69.84	84.12	55.90	75.46	82.57	53.53	79.44
log 16	86.25	60.81	66.12	84.12	55.84	75.48	81.82	52.53	81.01	79.52	49.94	84.79
baselines	accuracy 86.18			precision 69.41			recall 48.82					

Table 7: **Voting Accuracy, Teacher Precision, and Teacher Recall (in %) per Skew Personalization (Adult).** Average voting accuracy, teacher precision, and teacher recall over five voting processes by ten teacher ensembles using **upsampling** each for different budget distributions (higher budget & its ratio among minority data). Non-personalized experiments serve as baseline. The best voting accuracy is achieved at the higher budget log 4 with 25% ratio.

higher budget in $\epsilon$	accuracy (%)										
	min	25% ratio			50% ratio			75% ratio			max
		u	v	w	u	v	w	u	v	w	
log 4	84.51	88.68	60.18	88.21	90.44	78.83	90.78	91.94	88.58	91.70	92.40
		average			average			average			
log 8	84.51	90.56	0	90.40	92.44	82.42	92.34	93.30	90.84	93.39	94.01
		average			average			average			
log 16	84.51	91.57	0	91.39	93.56	85.85	93.27	94.31	92.78	94.28	94.76
		average			average			average			

Table 8: **Labels per Personalization with Multiple Baselines (MNIST).** Number of produced labels. Results depict the average over five voting processes by ten teacher ensembles each for different budget distributions and GNMax variants (**upsampling**, **vanishing**, **weighting**). Non-personalized experiments (with minimum, average, or maximum budget) serve as baselines. Due to inherent inefficiencies of vanishing PATE, no label could have been produced before exhaustion in two cases.

higher budget in $\epsilon$	accuracy (%)										
	min	25% ratio			50% ratio			75% ratio			max
		u	v	w	u	v	w	u	v	w	
log 4	79.85	81.02	76.17	80.87	81.76	78.62	81.76	82.16	80.70	82.26	82.52
		average			average			average			
log 8	79.85	81.79	75.73	81.67	82.52	79.32	82.60	82.87	82.09	82.89	83.02
		average			average			average			
log 16	79.85	82.30	75.31	82.25	82.82	79.97	82.84	83.07	82.72	83.04	83.23
		average			average			average			

Table 9: **Accuracy per Personalization with Multiple Baselines (Adult).** Number of produced labels. Results depict the average over five voting processes by ten teacher ensembles each for different budget distributions and GNMax variants (**upsampling**, **vanishing**, **weighting**). Non-personalized experiments (with minimum, average, or maximum budget) serve as baselines.

higher budget in $\epsilon$	accuracy (%)					
	min	25% ratio average	50% ratio average	75% ratio average	100% ratio average	max
log 4	79.85	81.26	81.41	81.35	80.57	82.52
log 8	79.85	81.51	80.72	78.60	77.78	83.02
log 16	79.85	81.39	78.74	77.36	76.24	83.23
		81.87	82.48	82.65	82.91	

Table 10: **Accuracy per Skew Personalization (Adult).** Number of produced labels. Results depict the average over five voting processes by ten teacher ensembles using **upsampling** each for different budget distributions (higher budget & its ratio among minority data). Non-personalized experiments with minimum, average, or maximum budget serve as baselines.